

# Analyst

Accepted Manuscript



This is an *Accepted Manuscript*, which has been through the Royal Society of Chemistry peer review process and has been accepted for publication.

*Accepted Manuscripts* are published online shortly after acceptance, before technical editing, formatting and proof reading. Using this free service, authors can make their results available to the community, in citable form, before we publish the edited article. We will replace this *Accepted Manuscript* with the edited and formatted *Advance Article* as soon as it is available.

You can find more information about *Accepted Manuscripts* in the [Information for Authors](#).

Please note that technical editing may introduce minor changes to the text and/or graphics, which may alter content. The journal's standard [Terms & Conditions](#) and the [Ethical guidelines](#) still apply. In no event shall the Royal Society of Chemistry be held responsible for any errors or omissions in this *Accepted Manuscript* or any consequences arising from the use of any information it contains.

**A how-to approach for estimation surface/Stern potentials considering ionic size and polarization**

Xinmin Liu, Feinan Hu, Wuquan Ding, Rui Tian, Rui Li, Hang Li\*

Chongqing key Laboratory of Soil Multi-scale Interfacial Process, College of Resources and  
Environment, Southwest University, Chongqing 400715, China

To whom correspondence should be addressed:

Email: [lihangswu@163.com](mailto:lihangswu@163.com) ;

Phone: 086-023-68251504

Fax: 086-023-68250444

**Abstract**

Potential in the electric double layer is an important parameter that significantly affects a large number of physical, chemical and biological properties and processes. In the present study, a new approach for estimation surface potential and Stern potential considering ionic volume and polarization was developed. Ionic strong polarization in the diffuse layer increases its effective charge and determines the Stern potential, while ionic volume in the Stern layer strongly decreases its effective charge and determines the surface potential. For example, the effective charge of  $K^+$  is increased by 0.699 (from 1 to 1.699) resulting from polarization, while that is decreased by 1.359 (from 1.699 to 0.240) due to finite size. The determined surface potential is about 7 times as high as the Stern potential. The effects of volume and polarization on surface/Stern potentials were quantified respectively, and the former stronger than the latter. The new theory was verified by the experiments for aggregates stability. The present work also showed only introduction the strong polarization into DLVO theory can describe the interactions of colloidal particles.

## 1 Introduction

Electrostatic potentials are directly related to adsorption and distribution of charged ionic species at the solid/liquid interface. Within the electric double layer (EDL), the potential decreases from the charged surface to the bulk solution as shown in Fig. 1. The surface potential is potential at origin plane of Stern layer, and the Stern potential is the potential at the onset of diffuse layer (Fig. 1).

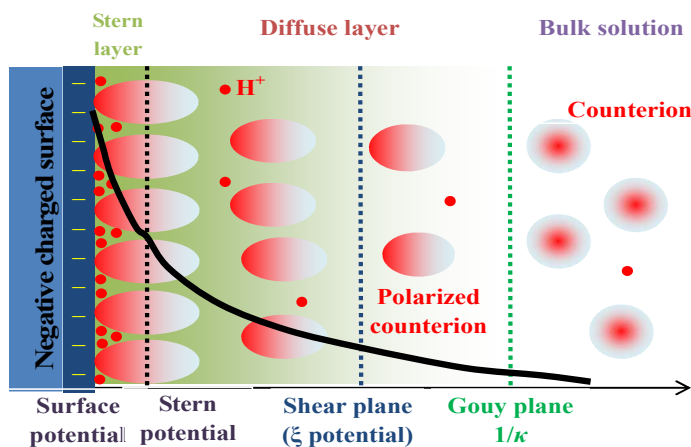


**Fig. 1** The schematic representation of potential (thick solid curve) and ion distribution in EDL. The thick red point represents hydrogen ion; the ellipses and circles represent the same species counterion with polarized counterion in EDL and unpolarized in bulk solution.

The EDL is fundamental for electrochemistry, colloidal and interface science, geotechnical and geoenvironmental engineering. Potential in the EDL has significant effects on a large number of physical, chemical and biological properties and processes. More importantly, the potential in the EDL (e.g. Stern potential, zeta potential) is determined by the surface potential and permittivity, Stern potential directly dominates the interfacial reactions and interactions between particles. Therefore, the estimation of surface potential and Stern potential of nano-colloidal particles in aqueous solution is a very important issue.

The estimation of surface potential was proposed by the Stern theory, which depends on the specific adsorption of counterions in the Stern layer.<sup>1,2</sup> Based on the Stern theory, the closest distance of counterions to the charged surfaces is limited by the finite size of the ions. The center charge of counterions is separated from the surface by a layer of thickness, i.e. Stern layer, in which there is no charge.<sup>3</sup> In the Stern layer, the electric potential drops linearly with distance from surface to the Stern plane.<sup>4</sup> Hydrogen ion could arrive at the Stern layer, since the hydration volume in Stern layer could be neglected.<sup>5</sup> Thus hydrogen ion of point charge obeys Boltzmann distribution both in the Stern layer and in the diffuse layer (Fig. 1). The permittivity in the Stern layer is much smaller than that in the diffuse layer, because the water molecules are strongly polarized by the high electrostatic attraction from the surface charges of colloidal particles<sup>6</sup>. However, these effects are neglected in theories of surface

potential determination, which usually leads to overestimate the surface potential.

Although many theories and methods have been developed to measure the Stern potential in the former studies,<sup>7-17</sup> the strong polarizations of counterions are always ignored leading to an overestimation of the Stern potential. It is well known that the surface charges of nano and colloid materials<sup>18-28</sup> could yield the strong electric field (usually  $10^8 \sim 10^9 \text{ V m}^{-1}$ ). Hence the adsorbed ions can be strongly polarized by such strong electric field, which could further increase the effective charge of ion and decrease the Stern potential. The relative difference of strong polarization between two counterions species was estimated in Stern potential determination<sup>20,28,29</sup> (called Stern potential as surface potential in these publications). However, the polarization of single counterion species is not quantified, which would lead to the determined Stern potential is also overestimated or underestimated. Moreover, the steric effects of inorganic ions could be neglected in the diffuse layer.<sup>30</sup> Therefore, the ionic strong polarization effects should be included in the current theories of electrostatic potential determination in EDL.

In the present study, we aim to develop a new approach for estimation surface potential and Stern potential considering the ionic size and polarization. The effective charges and polarization of counterions in EDL were quantified, and our new theory was also verified by the experiments. This work would help us to clearly understand the structure of EDL, the inner driven forces of colloidal aggregates stability.

## 2 Theory

The Poisson-Boltzmann equation (PBE) is:

$$\nabla^2 \varphi = -\frac{4\pi}{\varepsilon} \sum_i Z_i F f_i^0 e^{-Z_i F \varphi(\mathbf{r}) / RT} \quad (1)$$

where  $\pi$  is the circumference ratio,  $\varepsilon$  is the dielectric constant,  $Z_i$  is the valence of ion  $i$  species,  $a_i^0$  is the activity of ion  $i$  species in bulk solution,  $F$  is the Faraday constant,  $R$  is the gas constant,  $T$  is the absolute temperature,  $\varphi(\mathbf{r})$  is the potential distribution in diffuse layer.

In mathematically:

$$d\left(\frac{d\varphi}{dx}\right)^2 \equiv 2 \frac{d^2\varphi}{dx^2} d\varphi \quad (2)$$

Introducing Eq. (1) into Eq. (2) for a charged wall, we have:

$$\frac{d\varphi}{dx} = -\text{sgn}(y) \sqrt{\frac{8\pi RT}{\varepsilon} \sum_i f_i (\exp^{-Z_i F \varphi / RT} - 1)} \quad (3)$$

The potential distribution  $\varphi(x)$  was obtained by solving Eq. (3) at boundary condition,<sup>31</sup> and then introduction the  $\varphi(x)$  into Boltzmann equation gives the concentration profile  $f(x)$  in EDL. The mean ion concentration in EDL can be calculated based on Stern-Gouy-double-layer model. Hydrogen ion could

be regarded as a pointlike charge, the mean concentration of hydrogen ion in the Stern layer is:

$$\tilde{f}_{\text{H}_s} = \frac{N_{\text{H}_s}}{Sr} = \frac{1}{r} \int_0^r f_{\text{H}}(x) dx \quad (4)$$

Introduction Boltzmann equation into Eq. (4), and the ion-ion interactions<sup>20</sup> were considered (ion concentration is replaced by the activity), one gives:

$$Z_{\text{H}} F \varphi_s \approx 2RT \ln \left( \frac{2ra_{\text{H}}^0}{\sigma_{\text{H}_s}} \right) \quad (5)$$

where  $\sigma_{\text{H}_s}$  is the adsorption density of hydrogen ion in Stern layer,  $\sigma_{\text{H}_s} = N_{\text{H}_s}/S$ ,  $N_{\text{H}_s}$  is the adsorption number of hydrogen ion in Stern layer,  $S$  is the specific surface area of particles,  $r$  is the thickness of Stern layer,  $r = \sqrt{\frac{\varepsilon_s RT}{8\pi F^2 I}}$ ,  $\varepsilon_s$  is the mean dielectric constant in the Stern layer and  $\varepsilon_s \approx 6.67 \times 10^{-11} \text{ C}^2 \text{ J}^{-1} \text{ dm}^{-1}$ ,  $a_{\text{H}}^0$  is the activity of hydrogen ion.

The concentration of nonpoint ion in the Stern layer  $\tilde{f}_s$  equals 0. Equation (5) shows that the surface potential could be determined through adsorption equilibrium of hydrogen ion on nano-colloidal particles. Although adsorption density in the Stern layer  $\sigma_{\text{H}_s}$  could not be accurately determined, the total adsorption density  $\sigma_{\text{HT}}$  and adsorption density in the diffuse layer  $\sigma_{\text{Hd}}$  could be determined easily, thus  $\sigma_{\text{H}_s}$  could be calculated through the difference between  $\sigma_{\text{HT}}$  and  $\sigma_{\text{Hd}}$ .

The concentration of hydrogen ion in the diffuse layer is:

$$\tilde{f}_{\text{Hd}} = \frac{N_{\text{Hd}}}{V_d} = \frac{1}{\kappa} \int_r^{r+1/\kappa} f_{\text{H}}(x) dx \quad (6)$$

Introduction Boltzmann equation into Eq. (6) gives:

$$Z_{\text{H}} F \varphi_0 \approx 2RT \ln \left( \frac{Ma_{\text{H}}^0}{\sigma_{\text{Hd}} \kappa} \right) \quad (7)$$

where  $\kappa^{-1} = \sqrt{\varepsilon_w RT / (8\pi F^2 I)}$  is the thickness of diffuse layer,  $\varphi_0$  is the potential at the original plane of diffuse layer and  $\varphi_0 = \varphi(r)$ ,  $M$  is a function of counter-ionic concentrations in mixed electrolyte solutions, especially  $M=2$  in symmetric electrolyte solution,  $M=\sqrt{3}$  in 2:1 electrolyte solution and  $M=\sqrt{6}$  in 1:2 electrolyte solution,<sup>8</sup>  $M=0.5259 \ln(f_+^0/f_{++}^0)+1.992$  in 1:1+2:1 electrolyte solution ( $f_+^0$  and  $f_{++}^0$  is concentration of monovalent and bivalent counterions).<sup>28</sup>

Furthermore, ionic polarization was found to strongly affect the adsorption of counterions in the double layer on a charged surface.<sup>32,33</sup> The analytical solution of PBE cannot be derived when ion polarization is involved, thus here the ion polarization is involved in energy term of the analytical solution based on the classical PBE. The ions except hydrogen ion could be regarded as nonpoint charges, thus they could be taken as no adsorption in the Stern layer, i.e. the mean concentrations in Stern layer equal zero. For other ions, Eq. (7) is expressed as:

$$Z_i F \varphi_0 \approx 2RT \ln \left( \frac{Ma_i^0}{\sigma_i \kappa} \right) \quad (8)$$

The total energy between ion and surface results from not only Coulomb energy, but also Ionic hydration, size,<sup>34</sup> dispersion force,<sup>5</sup> induction force, cavity energy<sup>35</sup> and image charge interactions<sup>36-38</sup> and ion-ion correlations<sup>39-41</sup> et al. The ionic steric effects are not significant in diffuse layer based on earlier study.<sup>30</sup> The ion-ion and ion-surface correlations may decrease the surface charge (even charge inversion) for relatively high surface charge density at very high ion concentration.<sup>39-41</sup> The polarization and dispersion effects play an important role only on the surface with low charge density or weak electric field. Thus the dispersion or induction interactions were stressed under high ion concentration (>0.1 mol L<sup>-1</sup>),<sup>42</sup> the electrostatic effects was strongly screened in electrolyte solutions. Although image force between ion and the air-water interface may be the dominating contribution at the low concentrations, this force may be much weaker at the clay-water interface. A more important and neglected force, the strong non-classical polarization, exists in ion-surface interactions, which was induced by the strong electric field from surface charges of nano-colloidal particles.<sup>33</sup> This polarization could decrease the surface and Stern potential. The ion size and some other non-electrostatic interactions were neglected in this study, which may result in slightly overestimates the contributions of the polarization. The adsorbed electron-inclusive ions could be strongly polarized in strong external electric field results from surface charges of nano colloidal particles. The polarization of ions is included and Eq. (8) could be rewritten as,<sup>33</sup>

$$Z_i F \varphi_0 - \tilde{p}_i \tilde{E} = 2RT \ln \left( \frac{Ma_i^0}{\sigma_i \kappa} \right) \quad (9)$$

where  $\tilde{E}$  is mean electric field strength in diffuse layer,  $\tilde{E} = d\varphi/dx \approx (\varphi_0 - \varphi_{1/\kappa})/(0 - 1/\kappa) = -\kappa\varphi_0$ ,  $\tilde{p}_i$  is the dipole moment of  $i$ th ion in diffuse layer.

Thus Eq. (9) is changed as:

$$Z_i F \varphi_0 + \tilde{p}_i \kappa \varphi_0 = \beta_i Z_i F \varphi_0 = 2RT \ln \left( \frac{Ma_i^0}{\sigma_i \kappa} \right) \quad (10)$$

where  $\beta_i = 1 + \tilde{p}_i \kappa / Z_i F$ , it is called effective charge coefficient in diffuse layer. The coefficient  $\beta$  reflects the intensity of polarization at identical ion strength.

Lithium ion is the smallest one for all non-valence electrons ions and its polarization is the weakest in inorganic cations, thus here we assume Li<sup>+</sup> has no polarization, i.e.  $\tilde{p}_{Li} \approx 0$ , one has:

$$Z_{Li} F \varphi_0 + \tilde{p}_{Li} \kappa \varphi_0 \approx Z_{Li} F \varphi_0 = 2RT \ln \left( \frac{Ma_{Li}^0}{\sigma_{Li} \kappa} \right) \quad (11)$$

Based on Eqs. (11) and (10), we can see that the effective charge coefficient of  $\text{Li}^+$   $\beta_{\text{Li}}$  is taken as 1. The  $\varphi_0$  can be determined for adsorption of  $\text{Li}^+$  in binary cation exchange. Introducing the obtained  $\varphi_0$  into Eq. (10) in  $\text{Li}^+/i$  exchange equilibrium, we can calibrate the effective charge coefficient or dipole moment of counterions. Conversely, the  $\varphi_0$  can be determined in other  $i/j$  ion exchange equilibrium when their effective charge coefficients were obtained.

Once the  $\varphi_0$  is determined accurately in  $\text{H}^+/i$  exchange equilibrium, the adsorption density of hydrogen ion in diffuse layer can be calculated from Eq. (7), and then the  $\sigma_{\text{HS}}$  in Eq. (5) could be calculated:  $\sigma_{\text{HS}} = \sigma_{\text{HT}} - \sigma_{\text{HD}}$ . The surface potential could therefore be determined using Eq. (5). The surface potential could be evaluated by the adsorption of nonpoint charge ion:

$$\Pi_i Z_i F \varphi_s = \beta_i Z_i F \varphi_0 \quad (12)$$

where  $\Pi_i = \beta_i \varphi_0 / \varphi_s = [1 + \tilde{p}_i \kappa / (Z_i F)] \varphi_0 / \varphi_s$  is called effective charge coefficient in the Stern layer,  $\sigma_i = N_i / S$ ,  $S$  is the specific surface area of particles.

The surface potential and Stern potential could be determined in  $i/j$  mixed counterionic solutions based on Eq. (12):

$$\begin{aligned} (\beta_i Z_i - \beta_j Z_j) F \varphi_0 &= (\Pi_i Z_i - \Pi_j Z_j) F \varphi_s \\ &= 2RT \left[ \ln \left( \frac{M a_i^0}{\sigma_i \kappa} \right) - \ln \left( \frac{M a_j^0}{\sigma_j \kappa} \right) \right] = 2RT \ln \left( \frac{\sigma_j a_i^0}{\sigma_i a_j^0} \right) = 2RT \ln(K_{j/i}) \end{aligned} \quad (13)$$

where  $K_{j/i}$  is the selectivity coefficient and  $K_{j/i} = a_i^0 N_j / a_j^0 N_i$ .

### 3 Materials and methods

H/K and H/Na exchange experiments were conducted under the conditions of  $T=298$  K in our study. Purified montmorillonite (from WuHuaTianBao mineral resources Co., Ltd. in Inner Mongolia, China) was used as the experimental material, and the specific surface area ( $S$ ) is  $731 \text{ m}^2 \text{ g}^{-1}$ .<sup>20</sup> The montmorillonite sample was H-saturated in advance by using  $0.1 \text{ mol L}^{-1}$  HCl and sieved through 0.25 mm sieve after dried at  $70^\circ\text{C}$  before adsorption study. At the low pH of 1.0, our preliminary experiments showed that before and after  $\text{H}^+$  treatment, no significant change for the montmorillonite structure was observed.<sup>43</sup>

Approximately 1 g of the H-saturated sample was weighed in the 150 ml triangle bottle, to which adding  $0.03 \text{ mol L}^{-1}$  KOH or NaOH solution 25 ml. The suspension sample was allowed to equilibrate for 48 hours with continuous shaking at 298 K in an incubator shaker, and then, a standard  $1 \text{ mol L}^{-1}$  HCl solution was used to adjust pH of the suspension (several drops). Then after shaking for another 12 hours, the suspension was at equilibrium with  $\text{pH}=3\sim 6$  approximately.



The exchange equilibrium suspensions were centrifuged (4500 rpm) for 10 minutes and the supernatant decanted into clean plastic tubes. The activities of  $H^+$ ,  $Na^+$  or  $K^+$  in bulk solution were determined through pH, Na- or K-ion selective electrodes respectively for each experiment. Using the obtained activity values of  $Na^+$  and  $K^+$ , the concentration of  $Na^+$  and  $K^+$  could be calculated with the iteration method based on the modified Debye-Hückel equation.<sup>20</sup>

## 4 Results and discussion

### 4.1 The calibration of $\beta$ values for different ion species on montmorillonite

Based on the Na/Li, K/Li, Na/Mg and Na/Ca exchange equilibrium on montmorillonite surface,<sup>20,44</sup> the relative charge coefficients  $\beta_{(re)}$  for different counterion composition were calculated (Table 1), and then the effective charge coefficient  $\beta$ , effective charge  $Z_{eff}=Z\beta$  and the dipole moments  $\tilde{p}_n$  for different ion species would be calculated by combining the  $\beta_{Li} = 1+p_{Li,K}/Z_{Li}F \approx 1$ . The relative charge coefficient reflects the relative adsorption strength between two ion species involved in exchange adsorption, while the effective charge coefficient reflects the apparent adsorption strength of a given ion species.

The data in Table 1 reflect the difference of polarization for ions. The larger  $\beta$  value represents the ionic stronger polarization in the diffuse layer induced by the electric field from surface charges. The contribution of polarization is quantified for each ion by the parameter  $\beta$ . The ratio of polarization and Coulomb effect ( $(Z_{eff}-Z)/Z \times 100\%$ ) is 11.0% for  $Na^+$ , 69.9% for  $K^+$ , 34.0% for  $Mg^{2+}$  and 103.4 % for  $Ca^{2+}$ . When the charge coefficient or dipole moment of counterion was calibrated, the Stern potential only depends on selectivity coefficient that could be easily obtained by cation exchange equilibrium experiments.

**Table 1** The coefficients  $\beta$  for some alkali and alkali earth metal ions on montmorillonite

| $i$ th ion | $j$ th ion | $Z_j$ | $\beta_{i(re)}$        | $\beta_{j(re)}$   | $\beta_i$ | $\beta_j$ | $Z_{jeff}$ |
|------------|------------|-------|------------------------|-------------------|-----------|-----------|------------|
| $Li^+$     | $Na^+$     | 1     | $0.948 \pm 0.016^{44}$ | $1.052 \pm 0.016$ | 1         | 1.110     | 1.110      |
| $Li^+$     | $K^+$      | 1     | $0.741 \pm 0.007^{44}$ | $1.259 \pm 0.007$ | 1         | 1.699     | 1.699      |
| $Na^+$     | $Mg^{2+}$  | 2     | $0.906 \pm 0.016^{44}$ | $1.094 \pm 0.016$ | 1.110     | 1.340     | 2.680      |
| $Na^+$     | $Ca^{2+}$  | 2     | $0.706 \pm 0.024^{20}$ | $1.294 \pm 0.024$ | 1.110     | 2.034     | 4.068      |

### 4.2 The calibration of $\Pi$ values for different ion species on montmorillonite

The Stern potential  $\varphi_0$  was determined through the exchange equilibrium of  $K^+$  using Eq. (10), and then introduction the obtained  $\varphi_0$  values into Eq. (7) calculates the adsorption density of  $H^+$  in diffuse layer  $\sigma_{Hd}$ . Table 2 shows that the adsorption ability of  $H^+$  is much larger than that of  $K^+$ , because the selectivity coefficient  $K_{H/K} = a_K^0 N_H / a_H^0 N_K \gg 1$ . The  $\sigma_{Hd}$  values are much smaller than  $\sigma_{HT}$  values, thus  $\sigma_{Hd}$  values could be neglected and  $\sigma_{Hs} \approx \sigma_{HT}$ . The surface potential  $\varphi_s$  was determined by Eq. (5) and then introduction the obtained  $\varphi_s$  values into Eq. (12) calculates the  $\Pi_K$  values.  $H^+$  could be regarded as a point charge, while  $K^+$  has finite size. Therefore, a large number of  $H^+$  could arrive at charged surface or Stern layer, while  $K^+$  are only adsorbed in the diffuse layer.

**Table 2** The  $\Pi_K$  is determined by H/K exchange equilibrium on montmorillonite

| $a_K^0$              | $a_H^0$ | $N_K$                | $N_H^*$ | $\sigma_K$        | $\sigma_{HT}$ | $\varphi_0$ | $\sigma_{Hd}$     | $\varphi_s$ | $\Pi_K$     |
|----------------------|---------|----------------------|---------|-------------------|---------------|-------------|-------------------|-------------|-------------|
| mmol L <sup>-1</sup> |         | mmol g <sup>-1</sup> |         | C m <sup>-2</sup> |               | V           | C m <sup>-2</sup> | V           |             |
| 15.5                 | 1.14    | 0.313                | 0.837   | 0.0413            | 0.1105        | -0.0531     | 0.001472          | -0.341      | 0.264       |
| 14.1                 | 0.308   | 0.343                | 0.807   | 0.0452            | 0.1066        | -0.0566     | 0.000459          | -0.403      | 0.239       |
| 13.2                 | 0.141   | 0.375                | 0.775   | 0.0495            | 0.1023        | -0.0602     | 0.000234          | -0.439      | 0.233       |
| 12.0                 | 0.066   | 0.408                | 0.742   | 0.0539            | 0.0979        | -0.0641     | 0.000123          | -0.473      | 0.230       |
| 11.3                 | 0.0494  | 0.443                | 0.707   | 0.0584            | 0.0934        | -0.0674     | 0.000102          | -0.484      | 0.236       |
| 10.6                 | 0.0402  | 0.453                | 0.697   | 0.0598            | 0.0920        | -0.0690     | 0.000088          | -0.492      | 0.238       |
| 10.4                 | 0.0366  | 0.399                | 0.751   | 0.0526            | 0.0992        | -0.0655     | 0.000076          | -0.501      | 0.222       |
| 8.92                 | 0.0208  | 0.495                | 0.655   | 0.0653            | 0.0864        | -0.0743     | 0.000056          | -0.518      | 0.244       |
| 8.34                 | 0.0201  | 0.514                | 0.636   | 0.0678            | 0.0840        | -0.0765     | 0.000058          | -0.517      | 0.251       |
| 6.54                 | 0.0055  | 0.550                | 0.600   | 0.0727            | 0.0791        | -0.0822     | 0.000020          | -0.574      | 0.243       |
|                      |         |                      |         |                   |               |             |                   |             | 0.240±0.012 |

\*The adsorption number of hydrogen ion  $N_H$  equal the difference between the surface charge number  $N_T$  and adsorption number of potassium ion  $N_K$ , i.e.  $N_H = N_T - N_K$ .

The surface potential is much larger than Stern potential. The effective charge coefficient of  $K^+$  increases because of the strong polarization effects in the diffuse layer (1.699 in Table 1), while that strongly decreases due to steric effects (0.240 in Table 2). The charge coefficient  $\Pi$  represents the combined effects of polarization and steric effects. Although ionic steric effects are non-significant in the diffuse layer for inorganic ions,<sup>30</sup> while they are extraordinarily important in the Stern layer because there is no amount of effective charge for nonpoint ions. It should be note that the hydration of hydrogen ion is neglected for the strong polarization of water molecules in charged surfaces, and the dielectric constant in Stern layer is much smaller than in the diffuse layer.<sup>1</sup>

Based on Eq. (12), we have  $\beta_K/\beta_j = \Pi_K/\Pi_j$ . The  $\beta_j$  values were showed in Table 1, thus the  $\Pi_j$  values for other ions can be calculated though the obtained  $\Pi_K$  value and the results are showed in Table 3.

**Table 3** The  $\Pi$  values for ions

| Ion   | H <sup>+</sup> | K <sup>+</sup> | Na <sup>+</sup> | Li <sup>+</sup> | Ca <sup>2+</sup> | Mg <sup>2+</sup> |
|-------|----------------|----------------|-----------------|-----------------|------------------|------------------|
| $\Pi$ | 1              | 0.240          | 0.157           | 0.141           | 0.287            | 0.189            |

In comparison to the data in Table 3 and Table 1, we can see that the effective charge for ions much decrease considering the steric effects, yet they increase when ion polarization was taken account. In addition, the steric effects are stronger than polarization effects. For example, the effective charge for  $K^+$  is increased by 0.699 (from 1 to 1.699) resulting from non-classical polarization of  $K^+$ , while that is decreased by 1.359 (from 1.699 to 0.240) due to finite size of  $K^+$ . Based on Eq. (12), we have  $\varphi_s/\varphi_0 = \beta_i/\Pi_i$ . Surface potential is therefore 7 times as high as the Stern potential. The dielectric constant in the Stern layer share the same value in the diffuse layer, which results in an inexact charge coefficient.<sup>45</sup> On

the other hand, the relative charge coefficient between counterions was used,<sup>46</sup> which leads to underestimate the difference between surface potential and Stern potential.

In order to verify the  $\Pi$  values of other ions in Table 3 from H/K adsorption equilibrium, we independently selected H/Na exchange on montmorillonite to determine the  $\Pi_{\text{Na}}$  values.

**Table 4** The  $\Pi_{\text{Na}}$  values determined by H/Na exchange equilibrium on montmorillonite

| $f_{\text{Na}}^0$    | $f_{\text{H}}^0$ | $a_{\text{Na}}^0$ | $a_{\text{H}}^0$ | $N_{\text{Na}}$      | $N_{\text{H}}$ | $\varphi_0$ | $\varphi_s$ | $\Pi_{\text{Na}}$ |
|----------------------|------------------|-------------------|------------------|----------------------|----------------|-------------|-------------|-------------------|
| mmol L <sup>-1</sup> |                  |                   |                  | mmol g <sup>-1</sup> |                | V           |             |                   |
| 21.9                 | 0.20             | 18.8              | 0.17             | 0.202                | 0.948          | -0.0553     | -0.452      | 0.136             |
| 19.0                 | 0.017            | 16.5              | 0.015            | 0.267                | 0.883          | -0.0710     | -0.571      | 0.138             |
| 16.1                 | 0.0045           | 14.1              | 0.0040           | 0.347                | 0.803          | -0.0866     | -0.629      | 0.153             |
| 11.5                 | 0.0007           | 10.3              | 0.0006           | 0.446                | 0.704          | -0.106      | -0.708      | 0.165             |
| 10.4                 | 0.0011           | 9.32              | 0.0010           | 0.416                | 0.734          | -0.105      | -0.684      | 0.170             |
|                      |                  |                   |                  |                      |                |             |             | 0.153±0.015       |

Table 4 shows that the  $\Pi_{\text{Na}}$  ( $= 0.153$ ) values by H/Na exchange equilibrium are agree well with the theoretical predictions ( $= 0.157$ ), which indicating that the results in Table 3 are reasonable.

#### 4.3 The surface potential and Stern potential in $j/\text{Li}$ mixed ion solutions

Once the  $\beta$  and  $\Pi$  values of ions were calibrated, the Stern potential and surface potential only depend on the selectivity coefficient based on Eq. (13), and the results are showed in Fig. 2 for  $j/\text{Li}$  cation exchange ( $j$  represents  $\text{Na}^+$ ,  $\text{K}^+$ ,  $\text{Ca}^{2+}$  and  $\text{Mg}^{2+}$ ). Because the adsorption ability of  $\text{Li}^+$  is the weakest among  $\text{Na}^+$ ,  $\text{K}^+$ ,  $\text{Ca}^{2+}$  and  $\text{Mg}^{2+}$ ,<sup>44</sup> thus each determined  $K_{j/\text{Li}}$  by experiments is larger than 1 and  $\text{Li}^+$  is used as a reference.

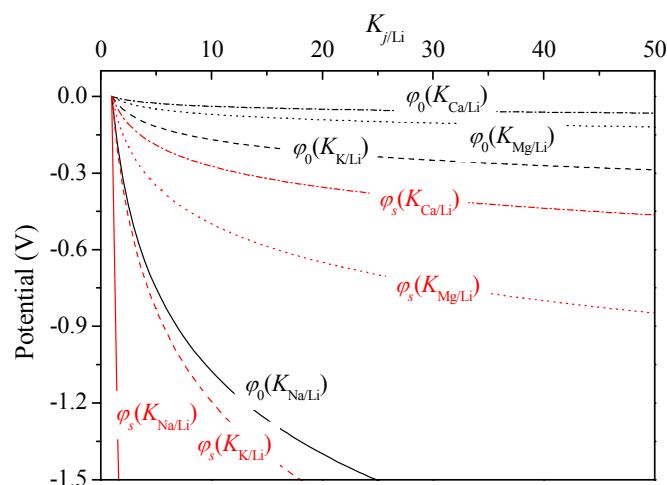


**Fig. 2** The surface potential and Stern potential as a function of selectivity coefficient  $K_{j/\text{Li}}$  in  $j/\text{Li}$  exchange

Figure 2 shows the surface potential is much larger than Stern potential. The selectivity coefficient was determined easily by cation exchange experiments, thus the surface and Stern potential can be

calculated. It is worth to note that the difference of effective charge coefficients is relatively small between  $\text{Li}^+$  and  $\text{Na}^+$ , thus the selectivity coefficient  $K_{\text{Na}/\text{Li}}$  is slightly larger than 1. Therefore, in actual applications, we suggest that  $\text{Na}^+$ - $\text{Li}^+$  group is not the best optimum to determine surface potential and Stern potential.

The electric potentials of model colloids were affected by the ion dispersion forces through Monte Carlo simulation study.<sup>47,48</sup> The ion specificity due to ion polarizability was strongly influenced by hydrated ion size. However, some researchers hold that the ions at near colloidal surface may be dehydration.<sup>5</sup> Furthermore, most of current researches underestimate the polarization contribution, which ignored the strong electric field at the surface.

The effective charge and selectivity coefficients have to be experimentally determined on montmorillonite surface, which is a phenomenological character. Based on our previous experiments, the prediction capability of the theoretical procedure is proved to be valid for nano  $\text{TiO}_2$  surface.<sup>20,29</sup> Therefore, we believe the new theory can also be extended to other colloidal particles.

#### 4.4 Application of the new theory to interactions between particles

Once the Stern potential was determined, the electrostatic repulsive pressure could be investigated based on the work of Langmuir.<sup>49</sup> The electrostatic repulsive interactions between colloidal particles strongly rely on potential at the overlapping position of two EDLs for the adjacent two particles. The relationship between potentials at midpoint of particles and at Stern plane could be derived from ref.:<sup>9</sup>

$$\left[ \frac{\pi}{2} - \arcsin e^{(ZF\phi_0 - ZF\phi_{d/2})/2RT} \right] \left[ \left( 1 + \frac{1}{4} e^{2ZF\phi_{d/2}/RT} + \frac{9}{64} e^{4ZF\phi_{d/2}/RT} \right) \right] = \frac{1}{4} d(\kappa + r) e^{-ZF\phi_{d/2}/2RT} \quad (14)$$

Although Eq. (14) was deduced from classical DLVO theory, the Stern potential determination includes the effects of ionic polarization and steric volume, thus we conclude that the specificity of colloidal particles interactions in different ion species could be quantified by the new theory. The potentials at midpoint of particles in different electrolyte solutions were determined and showed in Fig. 3. The differences of  $\phi_{d/2}$  in Fig. 3 result from ionic valence and polarization. Clearly, under the same electrolyte concentration, the series of  $\phi_{d/2}$  value (negative) is:  $\text{Li}^+ > \text{Na}^+ > \text{K}^+$ . when the  $\phi_{d/2}$  value was obtained, the electrostatic repulsive pressure could be calculated:<sup>49</sup>

$$P_{\text{EDL}} = 2RTf^0 \left[ \cosh \left( \frac{F\phi_{d/2}}{RT} \right) - 1 \right] \quad (15)$$

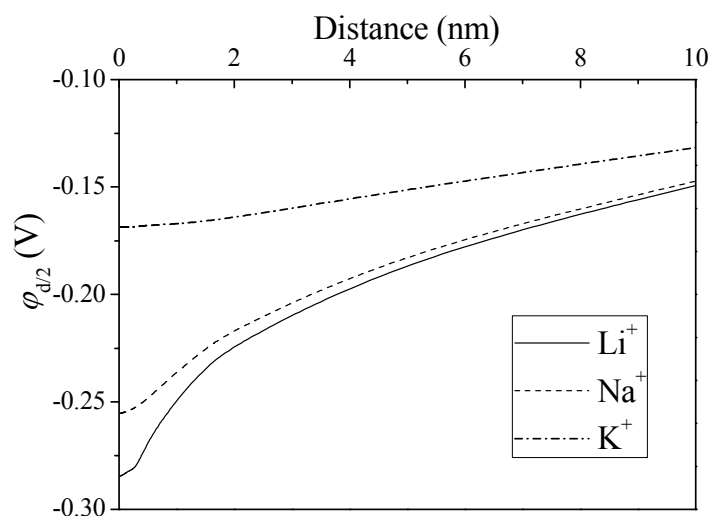


Fig. 3 The midplane potential between particles in different counterion system, the specific surface area of particle is  $73100 \text{ dm}^2 \text{ g}^{-1}$ , surface charge number is  $115 \text{ cmol}_{(c)} \text{ kg}^{-1}$ , concentration of electrolyte is  $0.0001 \text{ mol L}^{-1}$ .

Figure 4 shows the distribution of electrostatic repulsive pressure in different counterion system. From this figure it is clear to see that the electrostatic repulsive pressure in  $\text{Li}^+$  system is the largest, followed by  $\text{Na}^+$ , and  $\text{K}^+$  is last. The recent study demonstrated that particles interaction forces, especially the electrostatic force, are crucial for soil aggregate breakdown.<sup>50</sup> Therefore, based on the aforementioned theoretical analysis, when the electrostatic repulsive pressure shows the series of  $\text{Li}^+ > \text{Na}^+ > \text{K}^+$  at a given electrolyte concentration, we can infer that the stability of aggregate in corresponded system should show the order of  $\text{Li}^+ < \text{Na}^+ < \text{K}^+$ . Based on the theoretical analysis, we could predict the strength of aggregates breakdown in different cation species system, the series is:  $\text{Li}^+ > \text{Na}^+ > \text{K}^+$ . The experiments of montmorillonite aggregate stability in  $\text{LiNO}_3$ ,  $\text{NaNO}_3$  and  $\text{KNO}_3$  solution are showed in Fig. 5. The theoretical predictions agree with the experimental results in Fig. 5. In  $0.0001 \text{ mol L}^{-1} \text{ K}^+$  solutions, the largest electrostatic repulsive pressure at the separation 0 nm between two particles is only 1.7 atm (Fig. 4), which implies that the surface hydration force may be the first key process in aggregate breakdown. The content of released particles with different diameter is smallest in  $\text{KNO}_3$  solution (Fig. 5), because the surface hydration force could only be observed within a 2 nm between two adjacent particle surfaces.<sup>51</sup> Therefore, we can select the electrostatic repulsive pressure at the position of 2 nm distances from the surface quantify the strength of the aggregate breakdown. At this position, the electrostatic repulsive pressure in  $\text{K}^+$  solution is only 1.13 atm, in  $\text{Na}^+$  solution is 12.05 atm and in  $\text{Li}^+$  solution up to 16.16 atm (Fig. 4). The difference of  $P_{\text{EDL}}$  is 10.92 atm between  $\text{K}^+$  and  $\text{Na}^+$  solution and 15.03 atm between  $\text{K}^+$  and  $\text{Li}^+$  solution, corresponding the difference of  $< 2 \mu\text{m}$  breakdown strength is 37.32% and 39.19%, respectively. Similar to the change of  $< 5 \mu\text{m}$  and  $< 10 \mu\text{m}$ . The difference of  $P_{\text{EDL}}$  is

small (4.11 atm) between  $\text{Li}^+$  and  $\text{Na}^+$  solution results in the difference of  $< 2 \mu\text{m}$  breakdown strength is also small (1.87%).

Ion dispersion force has been regarded as an important factor that affects the interfacial potential and interactions of colloidal particles and become important especially when the electrolyte concentration is higher than about  $0.1 \text{ mol L}^{-1}$ .<sup>52,53</sup> However, the current experiments of aggregate breakdown showed that the difference of content of released particle between  $\text{Na}^+$  and  $\text{K}^+$  solutions is insignificant when the electrolyte concentration is higher than  $0.1 \text{ mol L}^{-1}$ .<sup>54</sup> It implies that ion dispersion force is not the main factor that affects the Stern potential, while the non-classical polarization force could well explain the experimental results. Therefore, we can reasonably expect that the new method of surface potential and Stern potential determination is valid. It also proves that only introduction the strong polarization into DLVO theory can describe the interactions of colloidal particles.

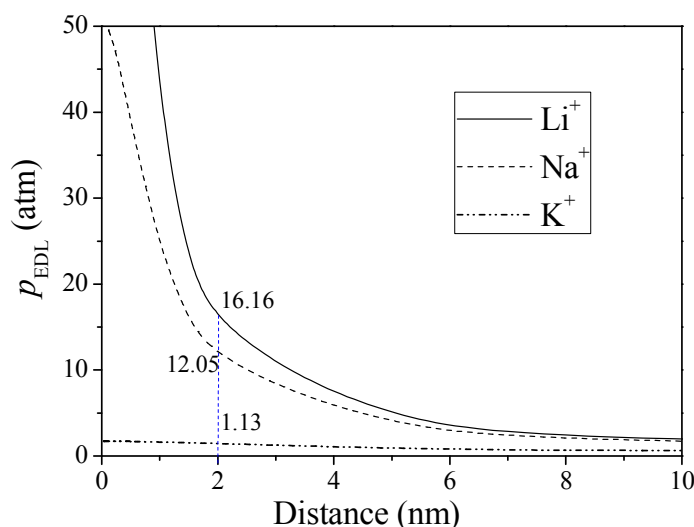


Fig. 4 The electrostatic repulsive pressure as a function of distance between adjacent particles in different electrolytes with  $0.0001 \text{ mol L}^{-1}$ .

The aggregation experiments performed by us are very simple and may be a weak proof about the applicability of the new theory. Although we tried to use the stability experiments of aggregation in the publication,<sup>55</sup> the charge density of these colloids are unknown, thus the Stern potential could not be calculated theoretically. However, we also use the laser scattering experiments independently test the validity of the new theory.<sup>56</sup> only the polarization effect can give a rational interpretation of the specific ion effects on colloidal particle aggregation.

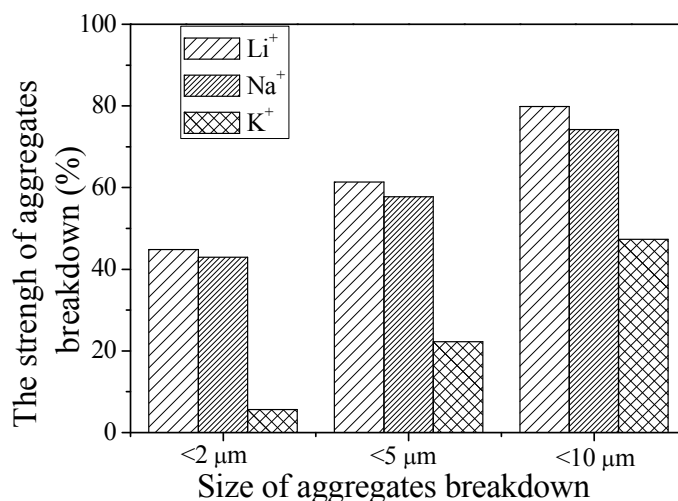


Fig. 5 The comparison of aggregates breaking strength with different diameter in LiNO<sub>3</sub>, NaNO<sub>3</sub> and KNO<sub>3</sub> electrolyte solutions with 0.0001 mol L<sup>-1</sup> respectively. The experimental data from the ref.<sup>57</sup>

## 5 Conclusions

A new theory and method for the surface potential and Stern potential was proposed in the present study while taking into account the ionic finite size and polarization. The effective charge coefficients were introduced to evaluate the contributions of ionic volume and polarization in the new theory. Since the polarization of Li<sup>+</sup> is weakest for non-valence electron ions, we assumed Li<sup>+</sup> has no polarization, i.e. the effective charge for Li<sup>+</sup> equals its valence. Thereby the effective charge taking into account the ionic polarization for other cations could be calculated through the adsorption equilibrium between Li<sup>+</sup> and other cation species (e.g. Na<sup>+</sup> = 1.110, K<sup>+</sup> = 1.699, Mg<sup>2+</sup> = 2.680 and Ca<sup>2+</sup> = 4.068). The new theory showed that the Stern potential only depends on the effective charge of counterions and selectivity coefficient that could be determined easily by experiments. Hydrogen ion H<sup>+</sup> could be nearly regarded as a point charge and no polarization, which could transmit the signal in the Stern layer. According to the adsorption equilibrium between H<sup>+</sup> and other cation species, the effective charge for other ions considering the combination between the volume and polarization could be calibrated (e.g. Na<sup>+</sup> = 0.157, K<sup>+</sup> = 0.240, Mg<sup>2+</sup> = 0.378 and Ca<sup>2+</sup> = 0.574), and then the surface potential could be determined correspondingly.

The effective charge equals ionic valence when the ionic polarization and volume were neglected, while it is larger than valence resulting from ion strong polarization and it is much smaller than valence because of the ionic steric effects. The contributions of steric effects to the surface potential were much stronger than that of polarization to the Stern potential. The surface potential is about 7 times as high as Stern potential. The surface potential and Stern potential (negative values) increase with decreasing polarization of ions. The electrostatic repulsive pressure calculated from the determined Stern potential could correctly predict the experiment of aggregate stability. The new theory for Stern potential was verified by the current experiments. The present work showed only introduction the strong polarization



into DLVO theory can describe the interactions of colloidal particles.

### Acknowledgments

This work was supported by the National Natural Science Foundation of China (Grant Nos.41371249, 41501240 and 41501241), China Postdoctoral Science Foundation (2015M570762 and 2015M572430).

### References

- 1 A. Sridharan and P. V. Satyamurty, *Clays Clay Miner.*, 1996, **44**, 479-484.
- 2 J. Q. Shang, K. Y. Lo and R. M. Quigley, *Can. Geotech. J.*, 1994, **31**, 624-636.
- 3 H. van Olphen, *An introduction to clay colloid chemistry*, Interscience, New York, 1963.
- 4 P. C. Hiemenz and R. Rajagopalan, *Principles of Colloid and Surface Chemistry, revised and expanded*, CRC Press, 1997.
- 5 D. F. Parsons, M. Boström, P. L. Nostro and B. W. Ninham, *Phys. Chem. Chem. Phys.*, 2011, **13**, 12352-12367.
- 6 B. E. Conway, J. O. M. Bockris and I. A. Ammar, *Trans. Faraday Soc.*, 1951, **47**, 756-766.
- 7 X. Zhang, B. A. Grimes, J.-C. Wang, K. M. Lacki and A. I. Liapis, *J. Colloid Interface Sci.*, 2004, **273**, 22-38.
- 8 H. Li, C. L. Qing, S. Q. Wei and X. J. Jiang, *J. Colloid Interface Sci.*, 2004, **275**, 172-176.
- 9 J. Hou and H. Li, *Soil Sci. Soc. Am. J.*, 2009, **73**, 1658-1663.
- 10 N. Kallay, T. Preočanin and T. Ivšić, *J. Colloid Interface Sci.*, 2007, **309**, 21-27.
- 11 I. Borukhov, D. Andelman and H. Orland, *Phys. Rev. Lett.*, 1997, **79**, 435-438.
- 12 Z. Y. Tong, Y. J. Zhu and C. H. Tong, *Chin. Phys. B*, 2014, **23**, 038202.
- 13 B. Peng and Y. X. Yu, *J. Chem. Phys.*, 2009, **131**, 134703.
- 14 K. Wang, Y.-X. Yu and G.-H. Gao, *J. Chem. Phys.*, 2008, **128**, 185101.
- 15 Z. L. Sun, Y. S. Kang, Y. M. Kang and J. M. Song, *Chin. Phys. B*, 2014, **23**, 126401.
- 16 Y. X. Yu, J. Z. Wu and G. H. Gao, *J. Chem. Phys.*, 2004, **120**, 7223-7233.
- 17 E. C. Y. Yan, Y. Liu and K. B. Eisenthal, *J. Phys. Chem. B*, 1998, **102**, 6331-6335.
- 18 H. Boroudjerdi, Y. W. Kim, A. Najji, R. R. Netz, X. Schlagberger and A. Serr, *Phys. Rep.*, 2005, **416**, 129-199.
- 19 G. H. Bolt, *Soil Sci.*, 1955, **79**, 267-276.
- 20 X. Liu, H. Li, R. Li, R. Tian and C. Xu, *Analyst*, 2013, **138**, 1122-1129.
- 21 M. Mullet, P. Fievet, J. C. Reggiani and J. Pagetti, *J. Membr. Sci.*, 1997, **123**, 255-265.
- 22 M. Mao, D. Fornasiero, J. Ralston, R. S. C. Smart and S. Sobieraj, *Colloids Surf. A*, 1994, **85**, 37-49.
- 23 W. R. Bowen and H. Mukhtar, *Colloids Surf. A*, 1993, **81**, 93-101.
- 24 W. Smit and C. L. M. Holten, *J. Colloid Interface Sci.*, 1980, **78**, 1-14.
- 25 J. Barber, *Biochim. Biophys. Acta Bioenerg.*, 1980, **594**, 253-308.
- 26 T. B. Kinraide and P. Wang, *J. Exp. Bot.*, 2010, **61**, 2507-2518.
- 27 I. Dobrzynska, E. Skrzydlewska and Z. Figaszewski, *Bioelectrochem.*, 2006, **69**, 142-147.
- 28 H. Li, J. Hou, X. Liu and L. Wu, *Soil Sci. Soc. Am. J.*, 2011, **75**, 2128-2135.
- 29 R. Li, H. Li, X. Liu, R. Tian, H. Zhu and H. Xiong, *RSC Adv.*, 2014, **4**, 24671-24678.
- 30 X. Liu, H. Li, R. Li, R. Tian and C. Xu, *Commun. Theor. Phys.*, 2012, **58**, 437-440.
- 31 X. Liu, H. Li, R. Li and R. Tian, *Surf. Sci.*, 2013, **607**, 197-202.
- 32 D. Frydel, *J. Chem. Phys.*, 2011, **134**, 234704.
- 33 X. Liu, H. Li, R. Li, D. Xie, J. Ni and L. Wu, *Sci. Rep.*, 2014, **4**, 5047.
- 34 E. R. A. Lima, F. W. Tavares and E. C. Biscaia Jr, *Phys. Chem. Chem. Phys.*, 2007, **9**, 3174-3180.
- 35 Y. Levin, A. P. d. Santos and A. Diehl, *Phys. Rev. Lett.*, 2009, **103**, 257802.



- 1  
2  
3 36 R. Wang and Z.-G. Wang, *J. Chem. Phys.*, 2013, **139**, 124702.  
4 37 M. Boström, D. R. M. Williams and B. W. Ninham, *Langmuir*, 2001, **17**, 4475-4478.  
5 38 F. W. Tavares, M. Boström, E. R. A. Lima and E. C. Biscaia Jr, *Fluid Phase Equilib.*, 2010, **296**,  
6 99-105.  
7  
8 39 P. Attard, *J. Phys. Chem.*, 1995, **99**, 14174-14181.  
9 40 E. Wernersson, R. Kjellander and J. Lyklema, *J. Phys. Chem. C*, 2010, **114**, 1849-1866.  
10 41 R. Kjellander, *J. Phys.: Condens. Matter*, 2009, **21**, 424101.  
11 42 P. H. R. Alijó, F. W. Tavares and E. C. B. Jr, *Colloids Surf. A*, 2012, **412**, 29-35.  
12 43 X. Liu, H. Li, R. Li, R. Tian and J. Hou, *J. Soils Sed.*, 2012, **12**, 1019-1029.  
13 44 X. Liu, H. Li, W. Du, R. Tian, R. Li and X. Jiang, *J. Phys. Chem. C*, 2013, **117**, 6245-6251.  
14 45 X. Liu, G. Yang, H. Li, R. Tian, R. Li, X. Jiang, J. Ni and D. Xie, *RSC Adv.*, 2014, **4**, 1189-1192.  
15 46 H. Fan, Y. Zhao, X. Liu, H. Li, R. Li and Y. He, *Acta Pedologica Sinica*, 2015, **52**, 446-452.  
16 47 A. Martín-Molina, J. G. Ibarra-Armenta and M. Quesada-Pérez, *J. Phys. Chem. B*, 2009, **113**,  
17 2414-2421.  
18 48 M. Quesada-Pérez, R. Hidalgo-Álvarez and A. Martín-Molina, *Colloid. Polym. Sci.*, 2010, **288**,  
19 151-158.  
20 49 I. Langmuir, *J. Chem. Phys.*, 1938, **6**, 873-896.  
21 50 F. Hu, C. Xu, H. Li, S. Li, Z. Yu, Y. Li and X. He, *Soil Till. Res.*, 2015, **147**, 1-9.  
22 51 Y. Leng, *Langmuir*, 2012, **28**, 5339-5349.  
23 52 M. Boström, D. R. M. Williams and B. W. Ninham, *Phys. Rev. Lett.*, 2001, **87**, 168103.  
24 53 M. C. Gurau, S. M. Lim, E. T. Castellana, F. Albertorio, S. Kataoka and P. S. Cremer, *J. Am. Chem.*  
25 *Soc.*, 2004, **126**, 10522-10523.  
26 54 C. Xu, H. Li, F. Hu, S. Li, X. Liu and Y. Li, *Eur. J. Soil Sci.*, 2015, **66**, 615-623.  
27 55 T. López-León, M. J. Santander-Ortega, J. L. Ortega-Vinuesa and D. Bastos-González, *J. Phys.*  
28 *Chem. C*, 2008, **112**, 16060-16069.  
29 56 R. Tian, G. Yang, H. Li, X. Gao, X. Liu, H. Zhu and Y. Tang, *Phys. Chem. Chem. Phys.*, 2014, **16**,  
30 8828-8836.  
31 57 F. Hu, H. Li, X. Liu, S. Li, W. Ding, C. Xu, Y. Li and L. Zhu, *PLoS ONE*, 2015, **10**, e0122460.  
32  
33  
34  
35  
36  
37  
38  
39  
40  
41  
42  
43  
44  
45  
46  
47  
48  
49  
50  
51  
52  
53  
54  
55  
56  
57  
58  
59  
60